Cumhuriyet Sci. J., 46(4) (2025) 967-973
DOI: https://doi.org/10.17776/csj.1698209

Cumhuriyet Science Journal

| csj.cumhuriyet.edu.tr | Founded: 2002 ISSN: 2587-2680 e-ISSN: 2587-246X Publisher: Sivas Cumhuriyet University

Development of Sandwich AlN on PSS via Layered V/III Ratio Optimization

İsmail Altuntaş[1,2,a,*], Ferhan Kübra Özbakır [1,2,b]

[1]*Nanotechnology Engineering, Faculty of Engineering, Sivas Cumhuriyet University, Sivas, Türkiye.*

[2]*Sivas Cumhuriyet University Nanophotonics Application and Research Center-CUNAM, Sivas, Türkiye*

**Corresponding author*

Research Article

History
Received: 13/05/2025
Accepted: 28/11/2025

ABSTRACT

This study presents a comprehensive investigation into the effects of layer-by-layer V/III ratio optimization on the structural, optical, and morphological properties of AlN films grown on patterned sapphire substrates (PSS) using the PALE technique. A sandwich structure was designed by sequentially applying low and high ammonia flows. Among the samples, the two-layer Sample B, grown with a low V/III ratio followed by a high one, exhibited the best crystalline quality, as indicated by the narrowest peaks in rocking curve analyses. In contrast, Sample A, grown as a single layer with a low V/III ratio, maintained the substrate's pattern geometry but showed increased structural irregularities due to limited vertical growth. Sample C, despite having a sandwich configuration, showed inferior surface and boundary morphology because the growth started under low ammonia flow, which negatively impacted crystalline alignment. Reflectance measurements revealed no significant shift in the band edge positions across the samples, indicating similar bandgap energies. However, the rougher surface morphology of Sample C led to slightly enhanced light scattering in the ultraviolet range, suggesting a less uniform optical surface. These findings demonstrate that carefully tuned V/III ratio sequencing—considering layer thickness and interface stability—can significantly enhance both the crystalline and surface quality of AlN/PSS heterostructures.

Keywords: AlN on PSS, MOVPE, HR-XRD, Spectrophotometer, SEM

[a] *ialtuntas@cumhuriyet.edu.tr* *https://orcid.org/0000-0002-3979-7868*
[b] *ferhan.k.ozbakir@msn.com* *https://orcid.org/0000-0002-3691-7983*

Introduction

Aluminum nitride (AlN) is a crucial semiconductor material that serves as an ideal choice for high-temperature and high-power applications. With unique properties such as a wide energy band gap, high thermal conductivity, low dielectric constant, and chemical stability, AlN is widely used in optoelectronic and electronic devices [1,2]

AlN has a wide energy band gap of approximately 6.2 eV, making it suitable for UV LEDs and lasers. This wide band gap also allows AlN to be used in high-temperature applications. Additionally, AlN possesses high thermal conductivity, around 200 W/mK, which makes it a preferred material in applications critical for heat management [3,4]. Particularly in power electronics and high-frequency devices, AlN's ability to optimize heat distribution provides significant advantages. Furthermore, AlN's low dielectric constant facilitates its use in high-frequency applications, enhancing the performance of RF (radio frequency) and microwave circuits. The chemical stability of AlN allows it to resist many chemicals, making it usable in harsh environments, ensuring that it is a long-lasting and reliable material [1].

The application areas of AlN are quite extensive. It is commonly used in the production of UV LEDs and lasers, where its wide energy band gap allows for UV light emission, making it indispensable in optoelectronic applications [5]. In high-frequency devices, such as RF amplifiers and microwave transmission lines, AlN provides high-frequency performance, and its low dielectric constant enhances the efficiency of these devices. In power electronics applications, AlN's high thermal conductivity is utilized to optimize heat distribution, contributing to more efficient operation and longer lifespan of devices [6]. Additionally, AlN's piezoelectric properties enable its use in sensor applications, allowing for precise measurement and detection systems [7].

The substrates used for growing AlN thin films directly impact the quality of epitaxial growth. Commonly used substrates include silicon (Si), which is economical and widely available, offering good electrical conductivity [8,9]. However, the thermal expansion coefficient of silicon (Si) is incompatible with that of AlN, which may lead to cracking. Therefore, careful optimization of Si-based AlN films is required. Silicon carbide (SiC) serves as an ideal substrate for AlN due to its high thermal conductivity and chemical stability. Moreover, its similar thermal expansion coefficient helps reduce the risk of cracking [10]. Sapphire (Al_2O_3) offers good surface quality and high-temperature resistance during the AlN growth process, thereby enhancing the crystal quality. In addition to these substrates, the use of patterned sapphire substrates (PSS) has been frequently reported in the literature to improve the crystal quality, with favorable results [11–13].

The synthesis of high-quality, defect-free AlN requires advanced growth techniques and precise optimization of deposition parameters. Among the methods commonly employed—such as molecular beam epitaxy (MBE) and physical vapor deposition (PVD) techniques—metal–organic chemical vapor deposition (MOCVD) stands out as one of the most attractive approaches. MOCVD offers several key advantages: it enables large-area uniform growth, precise control of composition and thickness at the atomic scale, and the ability to achieve epitaxial films with excellent crystallinity. To enhance the quality of AlN films, various techniques such as Pulsed Atomic Layer Epitaxy (PALE), Epitaxial Lateral Overgrowth (ELO), and the use of patterned substrates are commonly employed.

MOCVD-PALE approach, integrated within the MOCVD process, enables highly controlled, layer-by-layer growth of AlN thin films. By alternating precursor pulses and precisely adjusting growth temperature, PALE suppresses island formation, enhances lateral growth, and reduces dislocation densities—making it particularly effective for achieving smooth, high-quality AlN on lattice-mismatched substrates [14].

During the epitaxial growth process, various growth parameters such as the V/III ratio, growth temperature, rotation, and pressure affect the quality of AlN films. The V/III ratio, which determines the crystal structure and surface morphology, is critical. Caban et al. reported that among the samples they grew at a reactor temperature of 1240 °C with a constant TMAl flow of 21.8 µmol/min and using different NH_3 flow strategies (constant, low, and linearly decreasing), the sample grown with a linearly decreasing NH_3 flow exhibited low surface roughness and high crystal quality. They noted that this method provided optimal structural properties particularly in the thickness range of 400 nm to 1 µm, and offered better lateral uniformity [15]. Çörekçi et al. grew AlN thin films with thicknesses of 340, 550, and 750 nm, using NH_3 flow rates of 125, 70, and 70 sccm, respectively, and labeled the samples as A, B, and C. They associated the pit-like surface morphology observed in sample A, which had a high NH_3 flow rate, with overly active nitrogen species and the resulting low surface mobility. They also reported that strain energy and limited Al adatom diffusion contributed to pit formation [15]. Yolcu et al. examined AFM images of four AlN samples (A–D) grown with a constant TMAl flow rate of 77 sccm and NH_3 flow rates of 750, 900, 1050, and 1200 sccm, respectively. They observed that at high ammonia flow rates, a large number of small islands formed due to reduced surface mobility of Al adatoms. They reported that this condition negatively affected the surface morphology [15][16].

In conclusion, AlN is an ideal material for high-temperature and power applications, with extensive usage across various fields. AlN thin films obtained through the MOVPE method can be optimized with carefully controlled parameters during the epitaxial growth process. The properties of AlN, its application areas, and the factors to consider during the growth process further expand the potential applications of this material. The development of AlN-based devices represents an important research area, both theoretically and practically, aiming to contribute to future technological advancements. This study investigates the relationship between the V/III ratio and the properties of AlN thin films, highlighting the potential applications of AlN films obtained through the MOVPE method.

Experimental

All samples used in this study were grown using the horizontal flow AIXTRON 200/4 RF-S metal-organic vapor phase epitaxy (MOVPE) system located at the Sivas Cumhuriyet University Nanophotonics Application and Research Center. The growth processes were carried out on conical patterned (honeycomb) sapphire substrates. As schematically illustrated in Figure 1, the distance between the apexes of the patterns was approximately 3.0 µm, the distance between the base boundaries was 0.4 µm, the pattern height was 1.6 µm, and the base diameter of the patterns was 2.6 µm. During the growth process, hydrogen (H2) and nitrogen (N2) were used as carrier gases, and the reactor pressure was kept constant at 50 mbar. Prior to starting the growth process, substrates were exposed to a hydrogen atmosphere at 1400 °C for 10 minutes to remove impurities such as water vapor and atmospheric pollutants. After desorption, the TMAl source was opened, and a flow rate of 14 sccm was maintained for 2 seconds. Subsequently, the nucleation layer was grown at 1080 °C and 50 mbar pressure, with simultaneous feeding of TMAl (14 sccm) and NH3 (1200 sccm).

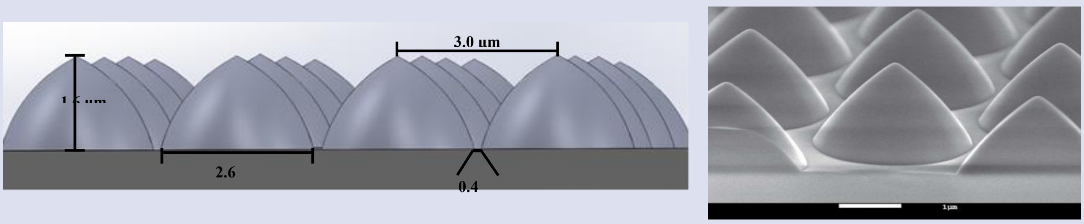

Figure 1. Schematic representation (a) and SEM images of the as-received substrate (b) of the honeycomb sapphire substrate, respectively

In this study, layered V/III ratio optimization was performed to obtain a sandwich AlN/PSS structure. A high V/III ratio of 1180 and a low V/III ratio of 590 were used. To achieve these values, the TMAl flow was kept constant at 77 sccm for all samples, while the NH_3 flow was set to 900 sccm for the high V/III ratio and 450 sccm for the low V/III ratio. For all three samples, one growth loop was defined as a 4 s TMAl flow followed by a 2 s NH_3 flow (**Hata! Başvuru kaynağı bulunamadı.**), the total number o f loops was set to 3600, with Sample A having 3600 loops (with low V/III ratio), Sample B having 1800*2 loops (with low and high V/III ratios) and Sample C having 1200*3 loops (with low, high, and low V/III ratios) (Figure 3). The characterizations of these three samples were conducted using a High-Resolution X-Ray Diffractometer (HR-XRD-Rigaku SmartLab), a Scanning Electron Microscope (SEM-Zeiss Sigma 300), and a UV-Vis-NIR Spectrophotometer (Varian Cary 5000).

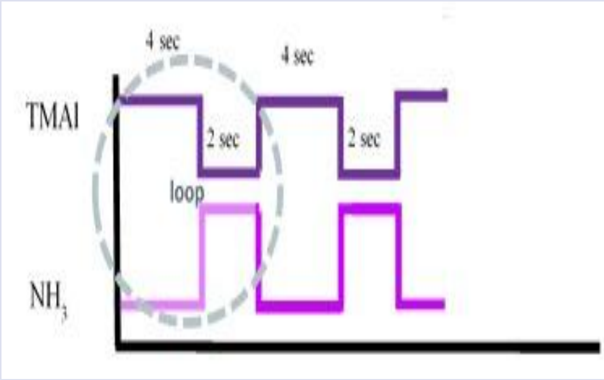

Figure 2. Schematic of one loop during the PALE-MOCVD growth method

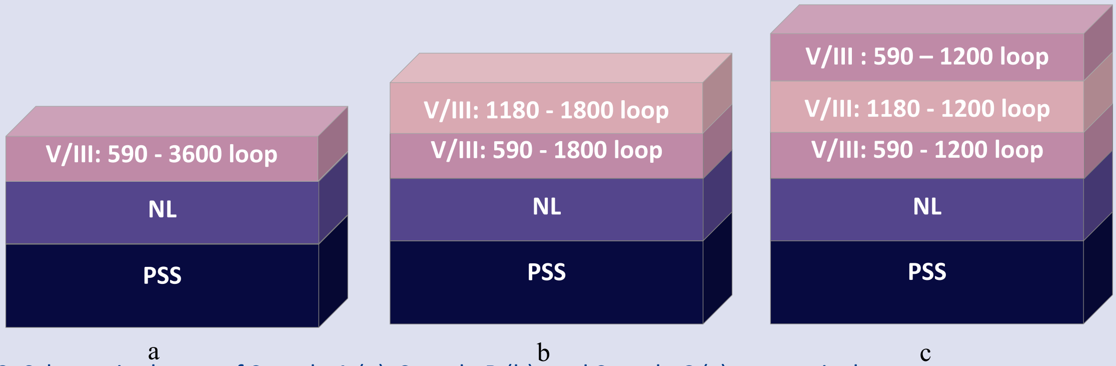

Figure 3. Schematic shapes of Sample A (a), Sample B (b), and Sample C (c), respectively

Result and discussion

It is known that low ammonia flow promotes lateral growth, while high ammonia flow supports three-dimensional (3D) growth [16]. In this study, a layer-by-layer V/III ratio optimization was performed to obtain a sandwich AlN/PSS structure, and the effects of this optimization on the structural, optical, and morphological properties of the samples were investigated. Figure 4 presents the bird's eye and cross-sectional SEM images of Sample A, Sample B, and Sample C, respectively. Considering the symmetric omega scan shown in Figure 6 and the asymmetric omega scan and the inset FWHM graph shown in Figure 7, it is observed that the two-layered Sample B, which was grown with a low V/III ratio followed by a high V/III ratio, exhibits superior crystal quality compared to Samples A and C, as evidenced by the narrower full width at half maximum (FWHM) values observed in both symmetric and asymmetric rocking curve profiles. In contrast, as shown in Figure 4, Samples A and C demonstrated more irregular growth behavior on the patterned substrate. In Sample A, which was grown as a single layer under low ammonia flow, the growth occurred over a narrower area of the patterns, preserving the honeycomb structure of the substrate (Figure 4.a.2). However, this limited vertical growth led to an increase in structural irregularities, thereby resulting in higher FWHM values. As shown in Figure 4.c.2, Sample C, which was grown in a sandwich structure starting with a low ammonia flow, exhibits a more irregular surface morphology and boundary structure compared to Samples A and B. These irregularities have led to a noticeable increase in the FWHM trend.

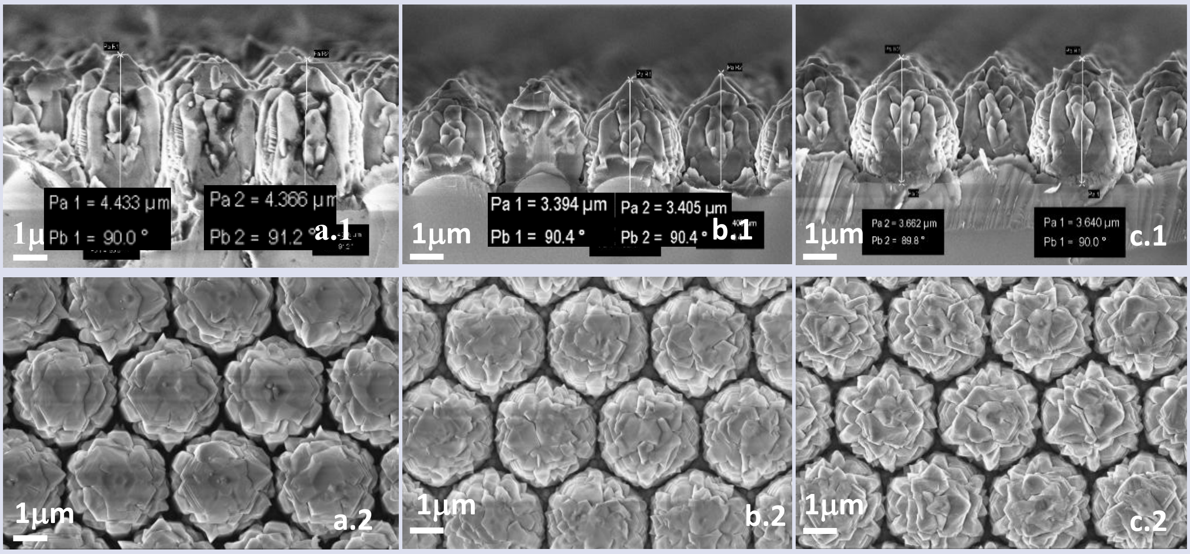

Figure 4. Cross-sectional SEM images (top row: a.1, b.1, and c.1), bird's-eye view SEM images (bottom row: a.2, b.2, and c.2) for Sample A, B, and C, respectively.

Sample B, which was grown as a two-layer structure with a low V/III ratio followed by a high one, demonstrated superior crystal quality with a narrower full width at half maximum (FWHM) trend in both symmetric and asymmetric rocking curve profiles. In contrast, the SEM images presented in Figure 4 show that Samples A and C exhibited more irregular growth behavior on the patterned substrate. Sample A, grown as a single layer under low ammonia flow, followed a narrower growth path along the patterns and preserved the honeycomb structure of the substrate (Figure 4.a.2). However, this vertical and limited growth led to an increase in structural irregularities, resulting in higher FWHM values. As shown in Figure 4.c.2, Sample C, which was grown in a sandwich structure starting with a low ammonia flow, exhibited a much more irregular particle surface and boundary morphology compared to Samples A and B because the ammonia flow was rapidly (1200 loops) changing during the sandwich growth before reaching equilibrium. This flow instability will reduce the interface quality thus degrading the crystal growth. In addition to the qualitative morphological evaluation, a quantitative analysis based on the cross-sectional SEM images was also performed. The island height was determined by measuring the vertical distance between the apex and the base of the islands shown in the Figure. Based on these measurements, the average island heights for Sample A, Sample B, and Sample C were calculated to be approximately 2.6 µm, 1.8 µm, and 1.6 µm, respectively.

In all samples, nucleation layers were formed under high ammonia flow, and epitaxial layers were grown on top with a total of 3600 loops. The formation of the nucleation layer under high ammonia flow reduced the surface adsorption of the Al precursor during TMAl supply [17]. This effect caused Sample A, which was grown under a low V/III ratio, to exhibit a significantly higher FWHM trend compared to the other samples.

Figure 5 presents the XRD 2θ-ω scan profiles of the c-plane AlN films grown on patterned sapphire substrates (PSS) for Sample A, B, and C. The prominent peak at 41.60° corresponds to the (006) reflection from the PSS. The (002) diffraction peak characteristic of c-plane AlN is observed at 36.05°, with no additional diffraction peaks detected, confirming that the c-plane AlN films are exclusively grown in a wurtzite hexagonal structure.

At low film thicknesses, the incomplete filling of gaps between growth islands hinders the formation of a smooth and crack-free surface. Therefore, changes in the V/III ratio at such low thicknesses destabilize the interface layers and degrade, rather than enhance, the crystal quality. SEM images support this observation, as Sample C shows greater surface roughness in the nucleation layers compared to Samples A and B. This roughness also results in a higher misorientation of crystal subregions in Sample C, as indicated by the broader FWHM values obtained from the asymmetric omega scan shown in Figure 7. The summarized XRD values are shown in Table 1.

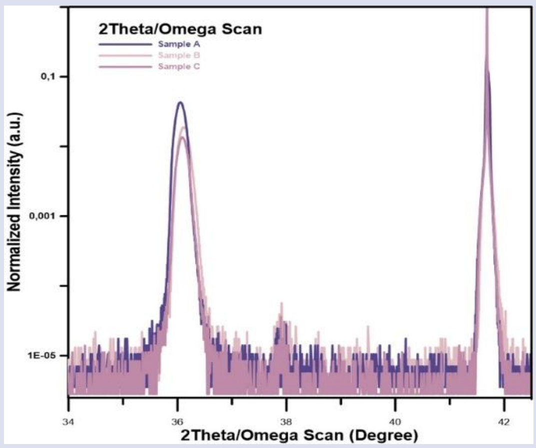

Figure 5. The comparison of the 2 Theta/Omega graphs of Sample A, B, and C.

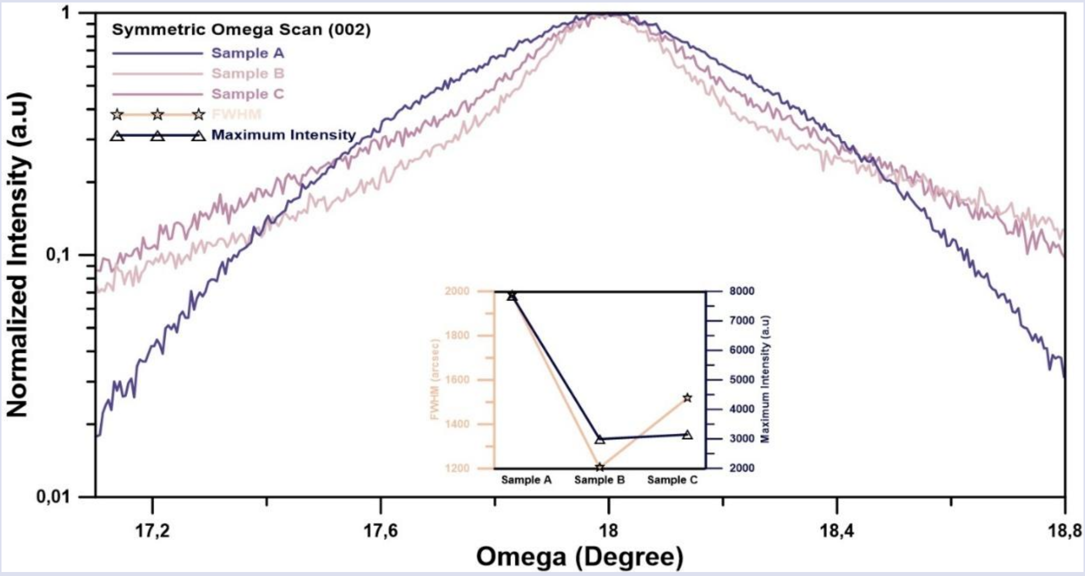

Figure 6. Symmetric rocking curve of samples.

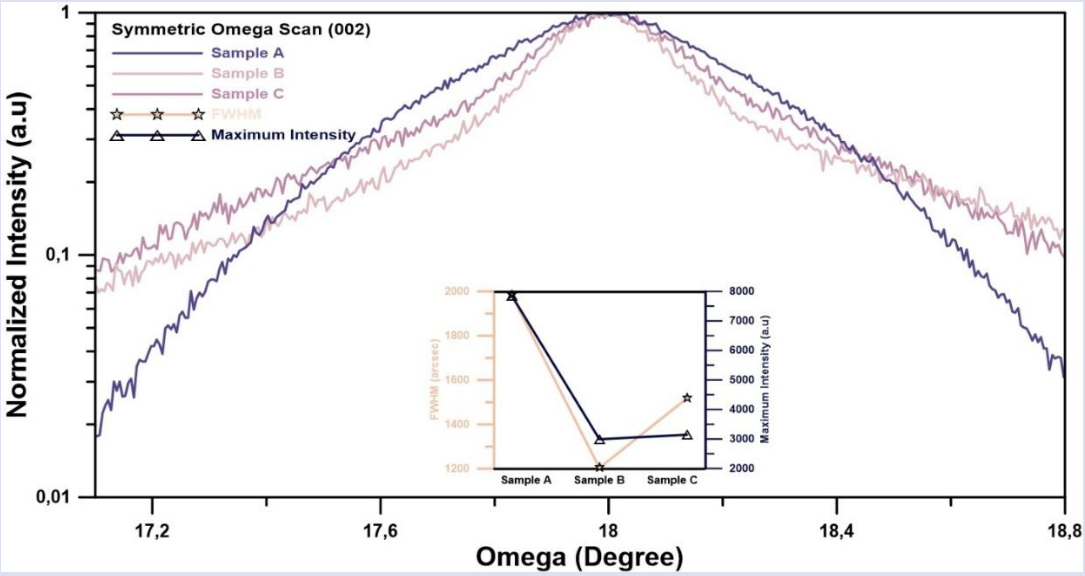

Figure 7. Asymmetric rocking curve of samples.

According to the spectral reflectance analysis presented in **Hata! Başvuru kaynağı bulunamadı.**, no s ignificant changes are observed at the absorption edges of the specular and diffuse reflectance curves for the three different samples. This indicates that the energy band transition regions of the samples are quite similar, and that the growth conditions used in this study do not directly affect the bandgap.

Table 1. FWHM and Maximum intensity values of symmetric and asymmetric omega scan

Samples	FWHM$_{(002)}$ (arcsec)	FWHM$_{(102)}$ (arcsec)	Max Intensity (002)	Max Intensity (102)
Sample A	1982	2078	7856	357
Sample B	1204	1720	2994	118
Sample C	1518	2127	3146	142

However, when focusing on Sample C, a noticeable increase in reflectance of approximately 1% around 300 nm, which corresponds to the ultraviolet (UV) region of the spectrum, is evident compared to the other samples. This increase is likely attributed to morphological differences on the surface of Sample C, which enhance the scattering effect of UV light. As described in Equation 1, the Kubelka-Munk function shows that reflectance is directly related to both the absorption and scattering coefficients. Although this increase may seem minor, it suggests that the surface of Sample C is optically less homogeneous, leading to increased scattering and consequently, variations in reflectance as reflected by the Kubelka-Munk function.

$$F(R) = \frac{(1-R)^2}{2R} = \frac{K}{S} \quad [18] \quad (1)$$

As described in Equation (1), the Kubelka–Munk function establishes a fundamental relationship between reflectance (R), the absorption coefficient (K), and the scattering coefficient (S). This theoretical framework is particularly useful in the analysis of diffuse reflectance spectra, as it allows the conversion of raw reflectance data into values that are more directly connected with the intrinsic optical properties of the material. According to this model, the reflectance is not only governed by the material's absorption behavior but also strongly influenced by its scattering characteristics.

In this context, the surface characteristics of Sample C have a more pronounced effect on the reflectance curves, particularly in the short wavelength (UV) range. Therefore, it can be concluded that Sample C exhibits lower performance in terms of surface uniformity and planarity compared to the other samples. Furthermore, the optical bandgaps of Sample A, B, and C were determined using Tauc's method (Figure 9). Among them, Sample B—exhibiting the lowest FWHM value and therefore the highest crystalline quality—showed the largest bandgap of approximately 5.67 eV, which is consistent with the obtained structural results.

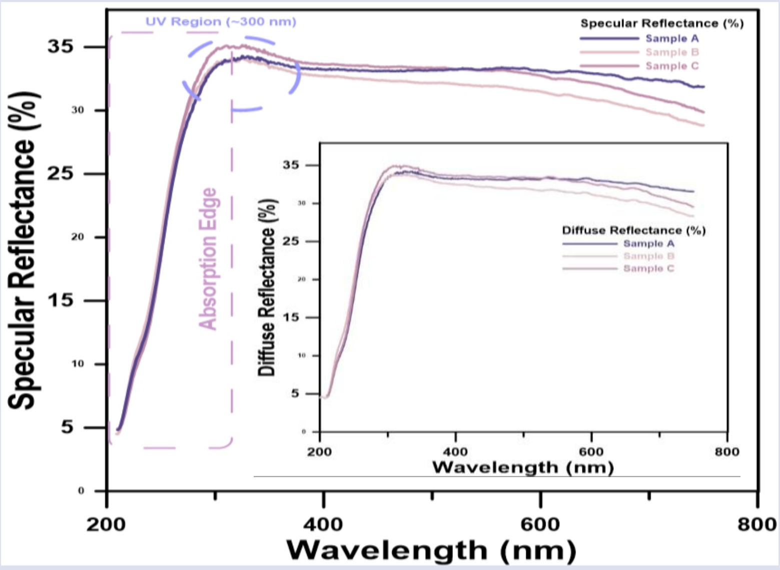

Figure 8. Specular and diffuse reflectance spectra of samples.

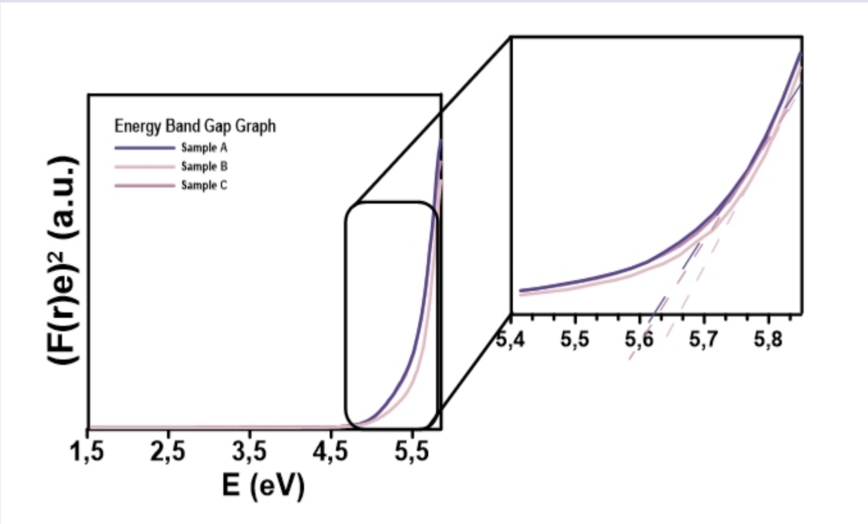

Figure 9. Bandgap graph of Sample A, B, and C.

Conclusion

In this study, a layer-by-layer V/III ratio optimization was performed to obtain a sandwich-structured AlN/PSS architecture, and the effects of this optimization on the structural, optical, and morphological properties of the samples were investigated. In particular, Sample B, grown with a two-layer configuration starting with a low and followed by a high V/III ratio, exhibited superior crystal quality, as evidenced by its lower FWHM values (1204 arcsec) in both symmetric and asymmetric rocking curve analyses.

Sample A, grown as a single layer under a low V/III ratio, showed limited vertical growth along the patterned substrate, preserving the underlying texture but resulting in increased structural irregularities and a broader FWHM value (1982 arcsec). Although Sample C was also grown with a sandwich structure, the initial use of a low ammonia flow led to surface and boundary irregularities. This was reflected in significantly broader FWHM values, particularly in asymmetric omega scans, indicating poorer crystal alignment.

According to the optical reflectance data, no significant variation was observed in the band edge positions among the samples. However, due to increased surface roughness, Sample C exhibited approximately 1% higher reflectance near 300 nm in the UV region. This behavior, interpreted via the Kubelka-Munk function, suggests enhanced light scattering due to surface inhomogeneity.

In conclusion, a controlled growth strategy involving sequential application of low and high V/III ratios—while also considering layer thicknesses and interface stability—emerges as the most effective approach for enhancing both crystal quality and surface uniformity in AlN/PSS structures.

Conflicts of interest

There are no conflicts of interest in this work.

Acknowledgements

This study was conducted within the Sivas Cumhuriyet University Nanophotonics Application and Research Center (CÜNAM) and is supported by TUBITAK-Turkey Scientific and Technological Research Council, under Project Number 118F425.

References

[1] Demir I, Li H, Robin Y, McClintock R, Elagoz S, Razeghi M. Sandwich method to grow high quality AlN by MOCVD. *Journal of Physics D: Applied Physics*, 51(8) (2018) 085104.

[2] Altuntas I, Kocak MN, Yolcu G, Budak HF, Kasapoğlu AE, Horoz S, Gür E., Demir I., Influence of the PALE growth temperature on quality of MOVPE grown AlN/Si (111*), Materials Science in Semiconductor Processing,* 127 (2021) 105733.

[3] Zhang Y, Long H, Zhang J, Tan B, Chen Q, Zhang S., Shan M., Zheng Z., Dai J., Chen C., Fast growth of high quality AlN films on sapphire using a dislocation filtering layer for ultraviolet light-emitting diodes, *CrystEngComm*, 21(27) (2019) 4072-4078.

[4] Isobe H, Kawamura F, Kawahara M, Yoshimura M, Mori Y, Sasaki T., Synthesis of AlN Grains and Liquid-Phase-Epitaxy (LPE) Growth of AlN Films Using Sn-Ca Mixed Flux. *Japanese journal of applied physics,* 44(4L) (2005) L488.

[5] Kneissl M, Kolbe T, Chua C, Kueller V, Lobo N, Stellmach J, et al. Advances in group III-nitride-based deep UV light-emitting diode technology. *Semiconductor Science and Technology,* 26(1) (2010) 014036.

[6] Du J, Dai W, Kou H, Wu P, Xing W, Zhang Y, et al. AlN coatings with high thermal conductivity and excellent electrical properties for thermal management devices. *CrystEngComm*, 21(27) (2019) 4072-4078.

[7] Lueng CM, Chan HLW, Surya C, Choy CL. Piezoelectric coefficient of aluminum nitride and gallium nitride. *Journal of applied physics*, 88(9) (2000) 5360-5363.

[8] Chen Z., Newman S., Brown D., Chung R., Keller S., Mishra U. K., Denbaars S., Nakamura,S., High quality AlN grown on SiC by metal organic chemical vapor deposition, *Applied Physics Letters,* (2008) 93(19).

[9] Perkitel İ., Altuntas İ., Demir İ., The Effect of Si (111) Substrate Surface Cleaning on Growth Rate and Crystal Quality of MOVPE Grown AlN, *Gazi University Journal of Science*, 35(1) (2022) 281-291

[10] Liu L, Liu B, Edgar J, … SR-J of applied, 2002 undefined. Raman characterization and stress analysis of AlN grown on SiC by sublimation. *Journal of applied physics*, *92*(9) (2002) 5183-5188.

[11] Conroy M, Zubialevich VZ, Li H, Petkov N, Holmes JD, Parbrook PJ. Epitaxial lateral overgrowth of AlN on self-assembled patterned nanorods. *Journal of Materials Chemistry C,* 3(2) (2015) p. 431-437.

[12] Chen Z, Hoo J, Chen Y, … VW-JJ of, 2019 undefined. Study of AlN based materials grown on nano-patterned sapphire substrates for deep ultraviolet LED applications. *Japanese Journal of Applied Physics,* 58(SC) (2019) p. SC1007.

[13] Lee D., Lee J., W., Jang J., Shin I., S., Jin L., Park J., H., Kim J., Jinsub L., Noh H., S., Kim Y., I., Park Y., Lee G., D., Park Y., Kim J., K., Yoon E., Improved performance of AlGaN-based deep ultraviolet light-emitting diodes with nano-patterned AlN/sapphire substrates. *Applied Physics Letters,* (2017) 110(19).

[14] Hisyam MI, Norhaniza R, Shuhaimi A, Mansor M, Williams A, Hussin MRM. Influence of Pulse Atomic-Layer Epitaxy (PALE) AlN Buffer Layer on Quality of MOCVD Grown GaN on Si(111) Substrate. *Surfaces and Interfaces* (2023);40:103041.

[15] Caban P, Rudzinski M, Wojcik M., Gaca J., Strupinski W., Growth of aluminium nitride with linear change of ammonia flow. *Journal of Crystal Growth,* 414 (2015) 81-86.

[16] Yolcu G, Koçak MN, Ünal DH, Altuntas I, Horoz S, Demir I. High-quality AlN growth: a detailed study on ammonia flow. *Journal of Materials Science: Materials in Electronics*, 34.4 (2023) 250.

[17] Simsek I, Yolcu G, Koçak MN, Pürlü K, Altuntas I, Demir I. Nucleation layer temperature effect on AlN epitaxial layers grown by metalorganic vapour phase epitaxy. *Journal of Materials Science: Materials in Electronics*, 32 (2021) 25507-25515.

[18] Takci DK, Senadim Tuzemen E, Kara K, Yilmaz S, Esen R, Baglayan O. Influence of Al concentration on structural and optical properties of Al-doped ZnO thin films. *Journal of Materials Science: Materials in Electronics,* 25 (2014) 2078-2085.